ISSN 2706-655X Vol. 8, Issue 2: 104-112, DOI: 10.25236/IJFET.2026.080213

Effect of Structure-Guided Single Mutant on Nicotinamide Coenzyme Specificity of Glucose Dehydrogenase from *Bacillus Megaterium*

Yujiao Shen, Keju Jing*

Department of Chemical and Biochemical Engineering, College of Chemistry and Chemical Engineering, Xiamen University, Xiamen, 361005, Fujian, China
jkj@xmu.edu.cn
**Corresponding author*

Abstract: *Glucose dehydrogenase (GDH) from Bacillus megateriumIWG3 is a NAD(P)$^+$-dependent oxidoreductase widely used in biosensing and biocatalytic NADPH regeneration. However, its intrinsic preference for NAD$^+$ over NADP$^+$ limits its application in NADPH-driven processes. Here, we report a structure-guided rational design to invert the coenzyme specificity of GDH by targeting a single residue within the conserved GXXXGXG motif of the Rossmann fold. Molecular docking and structural analysis identified Thr17 as the key residue forming a hydrogen bond with the 2'-hydroxyl of NAD$^+$, thereby discriminating against the 2'-phosphate of NADP$^+$. Three-point mutants—T17G, T17K, and T17R—were constructed, expressed, and kinetically characterized. The T17G mutation dramatically inverted cofactor preference, increasing the catalytic efficiency ratio (NADP$^+$/NAD$^+$) from 0.78 (wild-type) to 7.5, driven by a 2.4-fold decrease for NADP$^+$ and a 4.6-fold increase in for NAD$^+$. Remarkably, the T17K mutant not only shifted preference toward NADP$^+$ (specificity ratio 0.96) but also enhanced turnover numbers for both coenzymes by up to 5.2-fold, achieving catalytic efficiencies of 6.39 $mM^{-1}\cdot s^{-1}$ (NAD$^+$) and 6.15 $mM^{-1}\cdot s^{-1}$ (NADP$^+$)—the highest among all variants tested. In contrast, the T17R mutation severely impaired NADP$^+$ binding (k_m= 97.18 mM) and abolished activity. Structural modeling revealed that glycine creates space to accommodate the 2'-phosphate, while lysine establishes a favorable electrostatic interaction with the phosphate group; arginine's bulky guanidinium group causes steric clash. This study demonstrates that a single, rationally designed mutation at position 17 can simultaneously broaden cofactor specificity and improve catalytic efficiency, with the T17K mutant emerging as a superior biocatalyst for NADPH regeneration. The strategy provides a generalizable framework for engineering cofactor preference in short-chain dehydrogenase/reductase family enzymes.*

Keywords: *Glucose dehydrogenase; Cofactor specificity; Protein engineering; NADPH regeneration; Site-directed mutagenesis; Rossmann fold*

1. Introduction

Oxidoreductases constitute a major class of enzymes catalyzing redox reactions. Approximately 80% of these enzymes depend on nicotinamide adenine dinucleotide (NAD$^+$/NADH) as a coenzyme, while 10% utilize nicotinamide adenine dinucleotide phosphate (NADP$^+$/NADPH). A smaller fraction employs flavins (FMN, FAD) or coenzyme Q (PQQ). Structurally, NADP$^+$ differs from NAD$^+$ by a single phosphate group [1]; however, the cost of NADP$^+$ is approximately seven times higher than that of NAD$^+$. NAD(P)$^+$ serves as an electron carrier in redox reactions [2]. As the reaction proceeds, the substrate is oxidized, and NAD(P)$^+$ is reduced to NAD(P)H. To sustain the reaction, a continuous supply of NAD(P)$^+$ is required, yet the high cost of these coenzymes remains a major obstacle to the industrial-scale application of oxidoreductases. Consequently, developing efficient methods for NAD(P)H regeneration is critical.

Current methods for regenerating nicotinamide coenzymes include enzymatic, chemical, electrochemical, and photochemical approaches [3]. Due to its mild reaction conditions and high efficiency, enzymatic regeneration is the most commonly employed method. This approach involves adding a secondary enzyme and its substrate to establish a NAD(P)$^+$/NAD(P)H cycling system. While numerous enzymes are available for NADH regeneration, formate dehydrogenase remains the primary choice for NADPH regeneration [4]. This disparity highlights the research focus on tailoring coenzyme specificity for specific oxidoreductases.

ISSN 2706-655X Vol. 8, Issue 2: 104-112, DOI: 10.25236/IJFET.2026.080213

The seminal work by Richard N. Perham's team pioneered the successful reversal of cofactor preference [5]. Using molecular simulation and directed evolution, they modified the coenzyme specificity of glutathione reductase. Specifically, mutations at Arg198 and Arg204 disrupted the salt bridge between the enzyme and the 2'-phosphate of $NADP^+$. The resulting R198M/R204L mutant exhibited a 2.7-fold increase in affinity for NAD^+, though this came at the cost of reduced overall catalytic efficiency. Since then, research into coenzyme preference modification has flourished and can be broadly categorized into four types:

The first type focuses on switching coenzyme preference from NAD^+ to $NADP^+$. This is frequently investigated in formate dehydrogenase [6-10], where mutants with altered preference are developed for enhanced NADPH regeneration.

The second type aims to reverse the preference from $NADP^+$ to NAD^+ [11-15]. Numerous studies exist, employing diverse enzymes. For instance, the W1064S/R966D double mutant of *Bacillus megaterium* cytochrome P450 exhibited a dramatic shift in cofactor preference, with the catalytic efficiency ratio for $NADP^+$ over NAD^+ increasing from 810 to 10.5. Generally, mutating acidic residues (Asp, Glu) to basic ones (Arg, Lys) can switch coenzyme preference from NAD^+ to $NADP^+$ [16]. This is because acidic groups repel the negatively charged phosphate group on the $NADP^+$ ribose, whereas basic groups facilitate its binding.

The third type involves broadening coenzyme specificity, thereby enhancing catalytic efficiency for both $NAD(P)^+$ coenzymes [17]. For example, Elliot Campbell et al. (2010) engineered a thermostable alcohol dehydrogenase preferring $NADP^+$. Their single mutants K249G and H255R, and particularly the double mutant K249G/H255R, displayed significantly enhanced activity and broadened cofactor specificity.

The fourth type explores the transition between natural coenzymes and biomimetic analogs [18, 19]. The active site for hydride transfer in NAD(P) is the 1,4-dihydronicotinamide moiety [18, 20], while the adenosine diphosphate ribose portion primarily facilitates enzyme-coenzyme recognition [21]. This latter part can potentially be replaced with simpler groups for catalytic purposes [22]. The K249G/H255R double mutant of alcohol dehydrogenase showed a catalytic activity of 62×10^{-5} μM/min for the biomimetic coenzyme NMN^+, albeit with a catalytic efficiency for NAD^+ reduced by a factor of 645. Such mutants hold potential for applications like enzymatic biofuel cells [23], but current variants often suffer from low activity with biomimetic cofactors.

Computational strategies for altering coenzyme specificity have also been explored [24, 25]. A notable example is CSR-SALAD, a web-based tool for the universal reversal of nicotinamide cofactor specificity [26]. Built with Python, this database performs three tasks: structural analysis, design of cofactor-converting libraries, and active-site recovery. The last function addresses the issue of reduced catalytic activity post-mutation. Users can input a PDB file containing a cofactor-bound $NAD(P)^+$ structure for analysis, offering a general method for modifying nicotinamide cofactor specificity.

Glucose dehydrogenase (EC 1.1.1.47) is a short-chain dehydrogenase belonging to the alcohol dehydrogenase family [27] . It is widely used as a diagnostic enzyme for blood glucose monitoring and in biofuel cells. GDH is a homotetramer with a subunit size of approximately 28 kDa. It participates in the pentose phosphate pathway, utilizing $NAD(P)^+$ as a coenzyme to specifically catalyze the oxidation of D-glucose to β-D-gluconolactone (Figure 1).

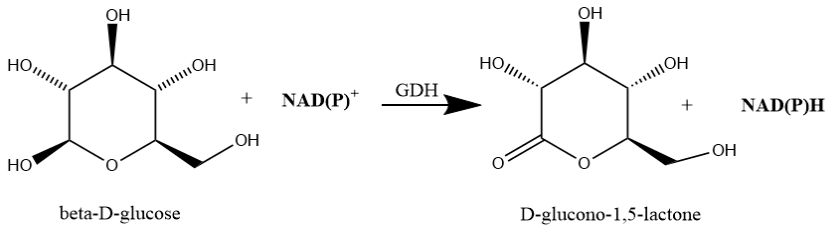

Figure 1. Reaction catalyzed by GDH.

The structure of GDH from *Bacillus megaterium* IWG3 was elucidated by Japanese researchers in 2001 [28]. A characteristic feature of this wild-type enzyme is its reversible pH-dependent dissociation: the tetramer dissociates into inactive monomers under alkaline conditions, which can reassemble into fully active tetramers upon lowering the pH to 6.5. The addition of 2 M NaCl prevents this alkaline dissociation, thereby stabilizing the tetrameric structure. The double mutant DN-46 (E170K, Q252L)

ISSN 2706-655X Vol. 8, Issue 2: 104-112, DOI: 10.25236/IJFET.2026.080213

exhibits exceptional thermostability without NaCl, with a half-life of 540 minutes at 66 °C, representing a 415-fold improvement over the wild-type enzyme.

GDH DN-46 [29, 30] is an NAD(P)$^+$-dependent dehydrogenase [29, 30], but it shows a marked preference for NAD$^+$ over NADP$^+$. Therefore, this study aims to alter the coenzyme preference of GDH to enable its efficient use in NADPH regeneration. A common theme across these studies is the identification of key residues influencing coenzyme preference through homologous recombination, followed by site-directed mutagenesis. These key residues are often those that form hydrogen bonds with the 2'-phosphate of NAD(P)$^+$ [31].

2. Materials and Methods

2.1 Bacterial Strains and Reagents

Primers were purchased from Sangon Co. Ltd (Shanghai, China) in PAGE-purified grade. *Escherichia coli*DH5α cells (ThermoFisher) were used for gene cloning and plasmid pET28a maintenance, while *E. coli* BL21(DE3) cells (TransGen) were employed for protein expression. Isopropyl β-D-thiogalactopyranoside (IPTG), NAD$^+$, and NADP$^+$ for enzyme activity assays were purchased from Sigma-Aldrich. All other chemicals were of analytical grade and obtained from commercial suppliers.

2.2 Molecular Docking Analysis

The crystal structure of GDH (PDB: 1RWB) was analyzed using the Discovery Studio (DS) molecular modeling system to identify amino acids interacting with the coenzyme NAD$^+$.

2.3 Site-Directed and Site-Saturation Mutagenesis of GDH

The gene encoding glucose dehydrogenase from *Bacillus megaterium* was cloned into the pET28a vector between the *NcoI* and *XhoI* restriction sites. The recombinant plasmid pET28a-GDH-N46 was used to express the wild-type (WT) enzyme and served as a template for introducing mutations. The Fast Mutagenesis System Kit (Qiagen) was used to introduce mutations at the cofactor-binding site T17.

Site-saturation mutagenesis was performed to generate a library of mutants at position 17. It has been reported that screening 88 clones is sufficient to cover all 20 amino acids at least once. The mutant library was transformed into *E. coli* BL21(DE3) cells, and 96 clones were selected for initial screening of NAD$^+$-dependent GDH activity. Positive clones were first screened on Luria-Bertani (LB) agar plates containing 50 μg/mL kanamycin. Subsequently, 96-well cell culture plates were used for further screening by measuring enzyme activity in cell lysates. Finally, positive clones were re-screened via shake-flask culture, and successfully verified mutants were sequenced by Shanghai Biotech.

2.4 Protein Expression and Purification of Wild-Type and Mutant Enzymes

*E. coli*BL21(DE3) cells transformed with WT or mutant GDH plasmids were used for recombinant protein expression. Single colonies were grown in LB medium containing 50 μg/mL kanamycin at 37 °C. Protein expression was induced with 0.3 mM IPTG when the OD_{600} reached 0.6–0.8, and the culture was incubated at 20 °C overnight. Cells were harvested by centrifugation and disrupted by sonication. The supernatant was purified using Ni-NTA resin affinity chromatography. Purified WT and mutant GDH were analyzed by SDS-PAGE and used for enzymatic assays. Protein concentration was determined using a BCA Protein Assay Kit with BSA as a standard.

2.5 Enzyme Activity Assays and Kinetic Parameters

Activities of wild-type and mutant enzymes were measured in 100 mM phosphate buffer (pH 7.0) containing 2 mM glucose and 2 mM NAD(P)$^+$ at 37 °C for 5 minutes. The formation of NAD(P)H was monitored at 340 nm using a UV/visible spectrophotometer. One unit of enzyme activity was defined as the amount of enzyme catalyzing the reduction of 1 μmol of NAD(P)$^+$ per minute. To determine kinetic parameters for the coenzyme, enzyme activity was measured under the same buffer conditions, varying the NAD(P)$^+$ concentration from 1 μM to 2 mM. Apparent K_m and k_{cat} values for NAD(P)$^+$ were calculated using nonlinear regression based on the Michaelis-Menten model. All experiments were

ISSN 2706-655X Vol. 8, Issue 2: 104-112, DOI: 10.25236/IJFET.2026.080213

performed in triplicate, and data were fitted within the linear range.

3. Results and Discussion

3.1 Structural Analysis of GDH

The crystal structure of glucose dehydrogenase from *Bacillus megaterium*IWG3 (PDB ID: 1RWB) was used as the template for molecular docking. The protein model was first prepared by adding hydrogen atoms and assigning proper protonation states at pH 7.0 using the Discovery Studio molecular modeling suite. The small-molecule ligand NAD^+ was energy-minimized with the CHARMm force field before docking.

Docking simulations were performed using the CDOCKER algorithm, and the top-ranked pose was selected based on binding energy and consistency with the known cofactor-binding mode of short-chain dehydrogenases. As shown in Figure 2, the docked complex reveals that the 2′-hydroxyl group of the NAD^+ adenine ribose is positioned within hydrogen-bonding distance (3.4 Å) of the side-chain hydroxyl of Thr17. Additionally, the backbone carbonyl of Thr17 forms a weak polar contact with the 3′-hydroxyl of the same ribose (distance 3.1 Å). These interactions are characteristic of the canonical Rossmann fold, where a conserved GXXXGXG motif (residues 14–20) forms a tight turn connecting the first β-strand (βA) and α-helix (αB). In this motif, the side chain of residue 17 projects directly into the cofactor-binding cleft.

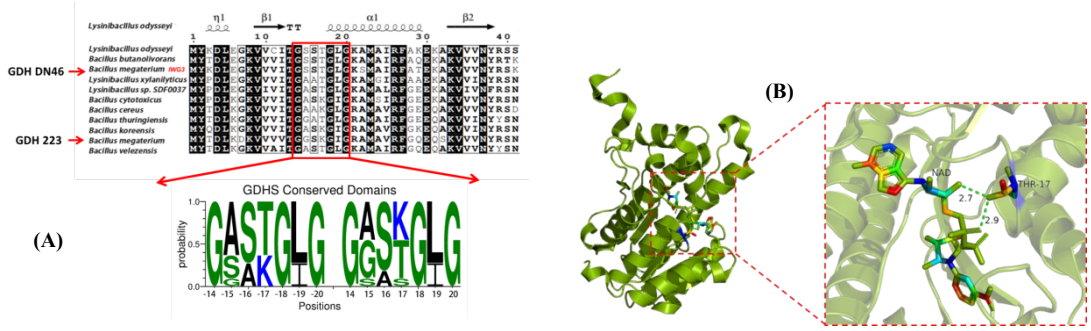

Figure 2. (A) Multiple sequence alignment of the cofactor-binding motifs of GDH and its 11 most closely related structures of the SDR family. The cofactor-binding GXXXGXG motif is boxed in red. (B) GlcDH structural analysis revealed a conserved residue (Thr17) that results in the hydrogen bond linking the 2′-phosphate of cofactor, which is one of key residues determining cofactor specificity. Threonine 17 is located in conserved GXXXGXG motif.

Beyond Thr17, several other residues within the binding pocket contribute to cofactor recognition. For instance, Asp37 (located in the second βαβ motif) forms a salt bridge with the ribose 2′-OH of the nicotinamide mononucleotide moiety, while Lys160 interacts with the pyrophosphate group. However, only Thr17 makes direct contact with the 2′-position that distinguishes NAD^+ from $NADP^+$. This unique spatial arrangement identifies Thr17 as the most promising target for engineering cofactor specificity.

To validate the docking result, we superimposed the docked NAD^+ onto the experimentally determined $NADP^+$-bound structure of a homologous glucose dehydrogenase from *Bacillus subtilis* (PDB: 3AY6). The overlay showed that the 2′-phosphate of $NADP^+$ would clash sterically with the methyl group of Thr17 (van der Waals overlap ~0.8 Å), confirming that mutation at this position is necessary to accommodate the larger phosphate group.

3.2 Expression and Purification of Mutant GDH

The recombinant plasmids encoding wild-type (WT) GDH DN-46 and the three mutants (T17G, T17K, T17R) were successfully constructed and verified by DNA sequencing. Each plasmid was transformed into *E. coli* BL21(DE3) cells, and protein expression was induced with 0.3 mM IPTG at 20 °C for 16 h. Under these conditions, all four variants were expressed predominantly in the soluble fraction, as judged by SDS-PAGE analysis of whole-cell lysates (Figure 3A).

After Ni-NTA affinity chromatography, the purified proteins appeared as a single major band at approximately 28 kDa on Coomassie-stained gels (Figure 3B), corresponding to the GDH monomer. No significant degradation products or contaminating bands were observed, indicating high purity (>95%)

ISSN 2706-655X Vol. 8, Issue 2: 104-112, DOI: 10.25236/IJFET.2026.080213

suitable for kinetic characterization. Typical yields were 15–25 mg of purified protein per liter of culture, with no substantial difference among the variants.

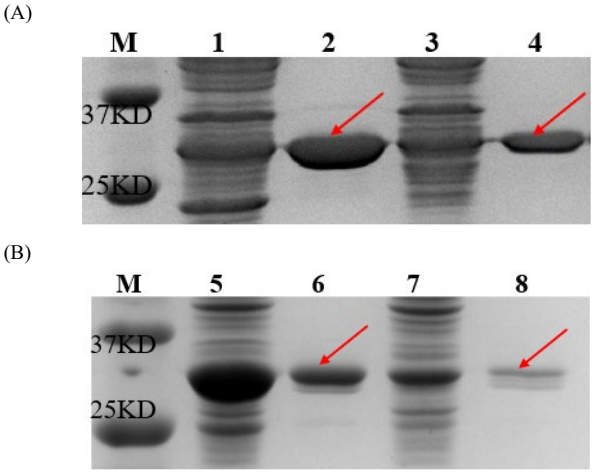

Figure 3. (A) Purification protein of recombination GDH. Purifying before (lane 1) and after (lane 2) of wild GDH protein and purifying before (lane 3) and after (lane 4) of mutant GDH T17G were analyzed by SDS-PAGE. (B) As shown in Figure 3A, Lane 5 and 6 are the SDS-PAGE of T17K before and after purification. Lane 7 and 8 are the SDS-PAGE of T17R before and after purification. The red arrows indicate the recombinant protein; M indicates the protein marker.

The oligomeric state of the purified enzymes was assessed by size-exclusion chromatography on a Superdex 200 Increase column. All four proteins eluted as a single symmetrical peak with an apparent molecular mass of ~110 kDa, consistent with the native tetrameric assembly. This confirms that the single-point mutations at position 17 do not disrupt the quaternary structure of GDH, which is essential for catalytic activity and stability.

3.3 Enzyme Activity and Determination of Kinetic Parameters

Steady-state kinetic parameters for the oxidation of glucose (20 mM fixed concentration) with varying concentrations of NAD^+ or $NADP^+$ (0–4 mM) were determined at 37 °C, pH 7.0. The initial velocity data were fitted to the Michaelis-Menten equation using nonlinear regression, yielding the values summarized in Table 1.

Table 1. Kinetic parameters of wild-type GDH and mutants toward NAD(P)$^+$.

Mutants	**K_m (mM)**		**K_{cat} (s^{-1})**		**K_{cat}/K_m ($mM^{-1}s^{-1}$)**		**Ratio K_{cat}/K_m**
	NAD^+	$NADP^+$	NAD^+	$NADP^+$	NAD^+	$NADP^+$	$NADP^+$/ NAD^+
WT	3.15±0.08	3.33±0.17	14.98±0.48	10.57±0.74	4.76±0.56	3.17±0.19	0.78
T17G	14.47±0.55	1.36±0.43	10.59±0.08	7.48±0.31	0.73±0.01	5.49±0.17	7.5
T17K	12.32±0.33	5.04±0.43	77.44±3.82	29.03±0.95	6.39±0.21	6.15±0.84	0.96
T17R	10.72±0.65	97.18±2.97	3.15±0.23	3.43±1.01	0.30±0.06	0.04±0.01	0.13

All enzymes were purified prior to characterization. Michaelis constants for cofactors were measured in the presence of saturating glucose concentrations (20 mM). Coenzyme concentrations ranged from 0 to 4 mM in 20 mM PBS buffer (pH 7.0). V_{max} is the maximum reaction rate. K_m and k_{cat} are the Michaelis constant and turnover number, respectively, for the GDH-catalyzed reaction with coenzyme $NAD(P)^+$.

As expected, the wild-type GDH DN46 showed a pronounced specificity for NAD^+. The K_m value for NAD^+ was 3.15 mM, while it was 3.33 mM for $NADP^+$. However, the single mutation T17G dramatically reduced the affinity for NAD^+ (K_m= 14.47 mM) while improving recognition of $NADP^+$ (K_m= 1.36 mM). This led to a 6.5-fold decrease in catalytic efficiency for NAD^+ but a 1.6-fold increase for $NADP^+$, ultimately resulting in an overall shift in coenzyme preference.

For the T17K mutant, coenzyme preference also shifted towards $NADP^+$, although the magnitude of change was less pronounced than for T17G. Importantly, the T17K mutant significantly improved catalytic efficiency for both coenzymes, with k_{cat}/K_m values of 6.39 $mM^{-1}\cdot s^{-1}$ and 6.15 $mM^{-1}\cdot s^{-1}$ for NAD^+ and $NADP^+$, respectively.

ISSN 2706-655X Vol. 8, Issue 2: 104-112, DOI: 10.25236/IJFET.2026.080213

Although both lysine and arginine are basic amino acids, the T17R mutant did not exhibit a similar change in preference for $NADP^+$. Instead, its catalytic efficiency decreased substantially, likely due to a sharp increase in its K_m value for $NADP^+$ (K_m= 97.18 mM) without a compensatory increase in k_{cat}. This resulted in a much lower catalytic efficiency ratio. These findings suggest that single mutants, such as T17K, may serve as effective tools for developing highly efficient reduced biocatalytic NADPH regeneration systems [32].

3.4 Interpretation of Coenzyme Preference Changes

Sequence alignment was performed using ESPript [33]. The NCBI database was used to compare the protein sequence of GDH DN46 with other glucose dehydrogenases from various sources. Many sequences exhibited over 90% sequence identity, which could confound the analysis. Therefore, CD-HIT was used to remove redundancy, retaining only one representative sequence from clusters with >90% identity. The secondary structure of GDH IWG3 (PDB ID: 1RWB) is shown at the top: α-helices are represented as squiggles, and β-strands as arrows.

As shown in Figure 4, alignment of GDH DN-46 with 30 homologous glucose dehydrogenases from diverse bacterial sources (after redundancy removal with CD-HIT at 90% identity cutoff) showed that the GXXXGXG motif (residues 14–20) is strictly conserved [33]. Within this motif, Thr17 is present in 80% of the sequences, while the remaining 20% contain serine or asparagine at the equivalent position. None of the natural homologs carry glycine, lysine, or arginine at this site, suggesting that the mutations we introduced are non-natural and likely to alter cofactor specificity.

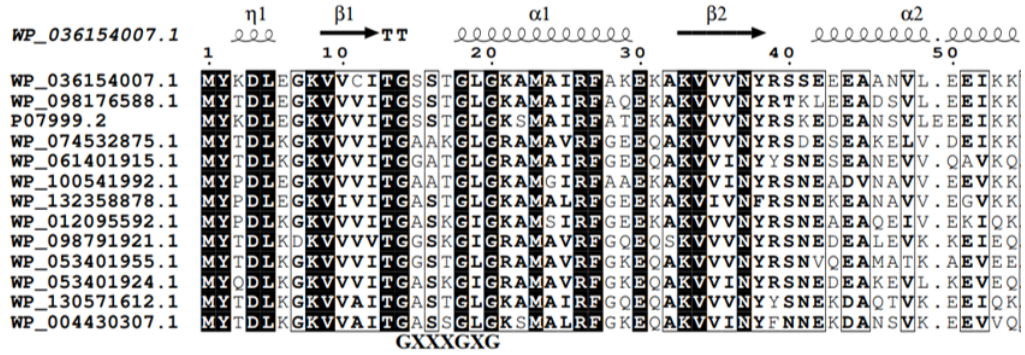

Figure 4. Multiple sequence alignment of GDH

To rationalize the observed kinetic changes at the molecular level, we performed sequence alignment and structural analysis using the ESPript server and PyMOL software.

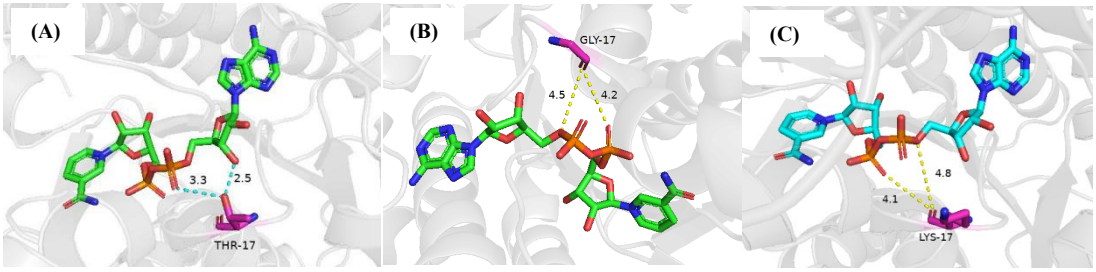

Figure 5. Key analysis of mutant GDH. PYMOL can be obtained by analyzing hydrogen bond formed by the mutant. It shows the combination of NAD and GDH residues. (A): the binding between WT and NAD(P)$^+$ 2′- phosphate acid. (B): the binding between mutant T17G and NAD(P)$^+$ 2′- phosphate. (C): the binding between mutant T17K and NAD(P)$^+$ 2′- phosphate. In the NAD structure, green is the carbon atom, blue is the nitrogen atom, red is the oxygen atom, and orangeis the phosphorus atom.

PyMOL was used to analyze the hydrogen-bonding networks in the modeled complexes of WT and mutant GDH with NAD(P)$^+$. In the WT structure (Figure 5A), the side-chain hydroxyl of Thr17 is 3.4 Å from the 2′-oxygen of the NAD^+ adenine ribose and 3.1 Å from the 3′-oxygen, forming two stabilizing hydrogen bonds. When Thr17 is replaced by glycine (Figure 5B), these hydrogen bonds are eliminated, and the backbone adopts a more flexible conformation. The absence of the side chain creates a cavity that accommodates the extra phosphate of $NADP^+$ without steric conflict. Moreover, the loss of the hydrogen bond with the 3′-OH may allow the ribose ring to rotate slightly, repositioning the 2′-phosphate

ISSN 2706-655X Vol. 8, Issue 2: 104-112, DOI: 10.25236/IJFET.2026.080213

into a more favorable orientation for binding.

For the T17K mutant (Figure 5C), the ε-amino group of lysine extends into the binding pocket and forms a new electrostatic interaction with the negatively charged 2′-phosphate of $NADP^+$. The distance between the NZ atom of Lys17 and the nearest oxygen of the phosphate is approximately 2.8 Å, indicative of a strong salt bridge. This interaction compensates for the loss of the original hydrogen bonds and stabilizes the enzyme–$NADP^+$ complex. In the case of NAD^+, the lysine side chain may interact with the 2′-OH through a weaker hydrogen bond or simply occupy space without causing repulsion, explaining why the catalytic efficiency for NAD^+ is actually improved.

The guanidinium group of arginine is planar, bulky, and capable of forming multiple hydrogen bonds. When placed at position 17, it likely protrudes too deeply into the cofactor-binding cleft, displacing the adenine ribose of $NADP^+$ from its optimal position. The increase of nearly 30-fold for $NADP^+$ suggests that the binding pocket is severely distorted. Additionally, the positive charge of arginine is delocalized over three nitrogen atoms, making it less effective at forming a directional salt bridge with the phosphate compared to the localized charge of lysine[26]. These geometric and electronic factors explain the poor performance of T17R.

Our results reinforce the concept that the residue at position 17 in the GXXXGXG motif acts as a gatekeeper for cofactor discrimination. A small neutral residue (glycine) favors $NADP^+$ by creating space, while a properly positioned basic residue (lysine) favors $NADP^+$ by providing electrostatic complementarity. Bulky basic residues (arginine) are detrimental. This knowledge provides a rational framework for engineering cofactor specificity in other members of the short-chain dehydrogenase/reductase (SDR) superfamily.

4. Conclusion

In this study, we employed a structure-guided rational design strategy to engineer the nicotinamide coenzyme specificity of glucose dehydrogenase (GDH) from *Bacillus megaterium* IWG3. Through molecular docking and structural analysis, Thr17 within the conserved GXXXGXG motif of the Rossmann fold was identified as a key residue governing cofactor discrimination. Three single-point mutants—T17G, T17K, and T17R—were constructed, purified, and kinetically characterized.

Our results demonstrate that a single amino acid substitution at position 17 can profoundly alter coenzyme preference, but the outcome is highly dependent on the chemical nature of the introduced side chain. The T17G mutation, which replaces threonine with a small, flexible glycine, effectively inverted cofactor specificity from NAD^+ to $NADP^+$, achieving a 7.5-fold increase in the catalytic efficiency ratio ($NADP^+/NAD^+$). This inversion is attributed to the elimination of steric hindrance and the creation of additional space that accommodates the 2′-phosphate group of $NADP^+$.

Notably, the T17K mutant exhibited a rare and practically valuable phenotype: it not only shifted cofactor preference toward $NADP^+$ (specificity ratio 0.96) but also substantially enhanced the catalytic efficiency for both coenzymes. The turnover numbers for NAD^+ and $NADP^+$ increased by 5.2-fold and 2.7-fold, respectively, relative to the wild-type enzyme. Structural modeling suggests that the positively charged ε-amino group of lysine forms a favorable electrostatic interaction with the negatively charged 2′-phosphate of $NADP^+$, while maintaining productive contacts with NAD^+. This dual improvement makes T17K a superior biocatalyst for flexible cofactor utilization.

In contrast, the T17R mutation proved detrimental, causing a 29-fold increase in $NADP^+$ and a drastic reduction in catalytic efficiency. The bulky and rigid guanidinium group of arginine introduces severe steric clash and suboptimal electrostatic geometry, underscoring that not all basic substitutions are functionally equivalent.

Collectively, this work establishes a clear structure–function relationship for residue 17 in GDH and provides a rational framework for engineering cofactor specificity in the short-chain dehydrogenase/reductase (SDR) superfamily. The T17K mutant, combining enhanced activity, broadened specificity, and preserved thermostability (inherited from the parental DN-46 scaffold), emerges as a promising candidate for efficient NADPH regeneration in biocatalytic cascades, such as the synthesis of chiral alcohols and other NADPH-dependent transformations. Future studies may explore combinatorial mutagenesis at adjacent positions (e.g., Asp37, Lys160) to further optimize selectivity, and structural determination of the T17K–$NADP^+$ complex by X-ray crystallography would provide definitive validation of the proposed binding mode.

ISSN 2706-655X Vol. 8, Issue 2: 104-112, DOI: 10.25236/IJFET.2026.080213

Acknowledgments

The authors gratefully acknowledge the financial support provided by the Natural Science Foundation of Fujian, China (No. 2023J01019).

References

[1] C. You, R. Huang, X. Wei, Z. Zhu, Y.P. Zhang, Protein engineering of oxidoreductases utilizing nicotinamide-based coenzymes, with applications in synthetic biology, Synth Syst Biotechnol, 2 (2017) 208-218.

[2] L. Selles Vidal, C.L. Kelly, P.M. Mordaka, J.T. Heap, Review of NAD(P)H-dependent oxidoreductases: Properties, engineering and application, Biochim Biophys Acta Proteins Proteom, 1866 (2018) 327-347.

[3] H. Wu, C. Tian, X. Song, C. Liu, D. Yang, Z. Jiang, Methods for the regeneration of nicotinamide coenzymes, Green Chemistry, 15 (2013) 1773.

[4] Z. Xu, K. Jing, Y. Liu, P. Cen, High-level expression of recombinant glucose dehydrogenase and its application in NADPH regeneration, Journal of industrial microbiology & biotechnology, 34 (2007) 83-90.

[5] A.B.R.N.P. Nigel S. Scrutton, Redesign of the coenzyme specificity of a dehygrogenase by protein engineering., nature, (1990).

[6] A. Andreadeli, D. Platis, V. Tishkov, V. Popov, N.E. Labrou, Structure-guided alteration of coenzyme specificity of formate dehydrogenase by saturation mutagenesis to enable efficient utilization of NADP+, FEBS J, 275 (2008) 3859-3869.

[7] S. Watanabe, T. Kodaki, K. Makino, Complete reversal of coenzyme specificity of xylitol dehydrogenase and increase of thermostability by the introduction of structural zinc, J Biol Chem, 280 (2005) 10340-10349.

[8] H. Zheng, D. Bertwistle, D.A. Sanders, D.R. Palmer, Converting NAD-specific inositol dehydrogenase to an efficient NADP-selective catalyst, with a surprising twist, Biochemistry, 52 (2013) 5876-5883.

[9] G.P. Ozgun, E.B. Ordu, H.E. Tutuncu, E. Yelboga, R.B. Sessions, N. Gul Karaguler, Site Saturation Mutagenesis Applications on Candida methylica Formate Dehydrogenase, Scientifica (Cairo), 2016 (2016) 4902450.

[10] W.A.v.d.D. Ryan Woodyer, and Huimin Zhao, Relaxing the Nicotinamide Cofactor Specificity of Phosphite Dehydrogenase by rational design123., Biochemistry, (2003) 11604-11614.

[11] K.R. Haiching Ma, |and Trevor M. Penning, Mutation of Nicotinamide Pocket Residues in Rat Liver 3R-Hydroxysteroid Dehydrogenase Reveals Different Modes of Cofactor Binding., Biochemistry, (2000).

[12] J.E. Carmen Pire, Juan Ferrer, Mar Bonete. Heterologous overexpression of glucose dehydrogenase from the halophilic archaeon Haloferax mediterranei., FEMS Microbiology Letter, (2001) 221-227.

[13] S. Banta, B.A. Swanson, S. Wu, A. Jarnagin, S. Anderson, Alteration of the specificity of the cofactor-binding pocket of Corynebacterium 2,5-diketo-D-gluconic acid reductase A, Protein Engineering, Design and Selection, 15 (2002) 131-140.

[14] C. Pire, J. Esclapez, S. Díaz, F. Pérez-Pomares, J. Ferrer, M.J. Bonete, Alteration of coenzyme specificity in halophilic NAD(P)$^+$ glucose dehydrogenase by site-directed mutagenesis, Journal of Molecular Catalysis B: Enzymatic, 59 (2009) 261-265.

[15] S. Bastian, X. Liu, J.T. Meyerowitz, C.D. Snow, M.M. Chen, F.H. Arnold, Engineered ketol-acid reductoisomerase and alcohol dehydrogenase enable anaerobic 2-methylpropan-1-ol production at theoretical yield in Escherichia coli, Metab Eng, 13 (2011) 345-352.

[16] A.M. Chanique, L.P. Parra, Protein Engineering for Nicotinamide Coenzyme Specificity in Oxidoreductases: Attempts and Challenges, Frontiers in microbiology, 9 (2018) 194.

[17] E. Campbell, I.R. Wheeldon, S. Banta, Broadening the cofactor specificity of a thermostable alcohol dehydrogenase using rational protein design introduces novel kinetic transient behavior, Biotechnol Bioeng, 107 (2010) 763-774.

[18] T. Knaus, C.E. Paul, C.W. Levy, S. de Vries, F.G. Mutti, F. Hollmann, N.S. Scrutton, Better than Nature: Nicotinamide Biomimetics That Outperform Natural Coenzymes, J Am Chem Soc, 138 (2016) 1033-1039.

[19] C. Nowak, A. Pick, P. Lommes, V. Sieber, Enzymatic Reduction of Nicotinamide Biomimetic Cofactors Using an Engineered Glucose Dehydrogenase: Providing a Regeneration System for Artificial Cofactors, ACS Catalysis, 7 (2017) 5202-5208.

[20] C.E. Paul, I.W.C.E. Arends, F. Hollmann, Is Simpler Better? Synthetic Nicotinamide Cofactor Analogues for Redox Chemistry, ACS Catalysis, 4 (2014) 788-797.

[21] M.Z. Erik Wernera, Felicitas Lernerb, Manfred Schweigerb, Udo Heinemann, Crystal structure of

ISSN 2706-655X Vol. 8, Issue 2: 104-112, DOI: 10.25236/IJFET.2026.080213

human nicotinamide mononucleotide adenylyltransferase in complex with NMN, FEBS Letters, (2002) 239-244.
[22] C.E. Paul, F. Hollmann, A survey of synthetic nicotinamide cofactors in enzymatic processes, Applied microbiology and biotechnology, 100 (2016) 4773-4778.
[23] E. Campbell, M. Meredith, S.D. Minteer, S. Banta, Enzymatic biofuel cells utilizing a biomimetic cofactor, Chem Commun (Camb), 48 (2012) 1898-1900.
[24] G.A. Khoury, H. Fazelinia, J.W. Chin, R.J. Pantazes, P.C. Cirino, C.D. Maranas, Computational design ofCandida boidiniixylose reductase for altered cofactor specificity, Protein Science, 18 (2009) 2125-2138.
[25] D. Cui, L. Zhang, S. Jiang, Z. Yao, B. Gao, J. Lin, Y.A. Yuan, D. Wei, A computational strategy for altering an enzyme in its cofactor preference to NAD(H) and/or NADP(H), The FEBS journal, 282 (2015) 2339-2351.
[26] J.K. Cahn, C.A. Werlang, A. Baumschlager, S. Brinkmann-Chen, S.L. Mayo, F.H. Arnold, A General Tool for Engineering the NAD/NADP Cofactor Preference of Oxidoreductases, ACS synthetic biology, 6 (2017) 326-333.
[27] Y.e. al, Crystallization and preliminary X-ray analysis of glucose dehydrogenase from Bacillus megaterium IWG3, crystallization papers, (2000) 1443-1445.
[28] G.K. Keizo Yamamoto, Masami Kusunoki, Shiro Tabata, Itaru Urabe, and Shigeyoshi Osaki, Crystal Structure of Glucose Dehydrogenase from Bacillus megaterium IWG3 at 1.7A Resolution., J. Biochem, (2001) 303-312.
[29] S.H. Baik, T. Ide, H. Yoshida, O. Kagami, S. Harayama, Significantly enhanced stability of glucose dehydrogenase by directed evolution, Applied microbiology and biotechnology, 61 (2003) 329-335.
[30] S.H. Baik, F. Michel, N. Aghajari, R. Haser, S. Harayama, Cooperative effect of two surface amino acid mutations (Q252L and E170K) in glucose dehydrogenase from Bacillus megaterium IWG3 on stabilization of its oligomeric state, Applied and environmental microbiology, 71 (2005) 3285-3293.
[31] S. Brinkmannchen, T. Flock, J.K. Cahn, C.D. Snow, E.M. Brustad, J.A. Mcintosh, P. Meinhold, L. Zhang, F.H. Arnold, General approach to reversing ketol-acid reductoisomerase cofactor dependence from NADPH to NADH, Pnas, 110 (2013) 10946-10951.
[32] A. Lerchner, A. Jarasch, A. Skerra, Engineering of alanine dehydrogenase from Bacillus subtilis for novel cofactor specificity, Biotechnol Appl Biochem, 63 (2016) 616-624.
[33] H.T. Ding, Y.Q. Du, D.F. Liu, Z.L. Li, X.J. Chen, Y.H. Zhao, Cloning and expression in E. coli of an organic solvent-tolerant and alkali-resistant glucose 1-dehydrogenase from Lysinibacillus sphaericus G10, Bioresour Technol, 102 (2011) 1528-1536.